Estimating Melatonin Suppression and Photosynthesis Activity in Real-World Scenes from Computer Generated Images

David Geisler-Moroder, Arne Dür; Department of Mathematics, University of Innsbruck, Austria

Abstract

In lighting design and architectural illumination planning simulations of luminance and illuminance distributions within scenes are performed using rendering tools such as RADIANCE. *In this paper we focus on the evaluation by two action spectra other than the luminous efficiency function – the circadian action function describing the melatonin suppression and the photosynthesis action function. We show how indices that are derived from these action spectra can be calculated from spectrally rendered images of a real-world scene. For both action spectra we derive approximations based on the CIE color matching functions that allow estimations of the corresponding index from RGB rendered images. We evaluate the differences between the spectral results and the RGB approximations for an office room with three different types of illumination.*

Background

Physically based rendering packages such as RADIANCE are used in lighting design and architectural illumination planning for simulations of luminance and illuminance distributions. Especially for daylight simulations and daylight factor calculations this rendering tool is widely used and was shown to be accurate in [1, 2, 3]. However, spectral rendering is necessary if highly accurate results are desired as for example color shifts may occur when calculations are performed in the RGB color space [4, 5].

In the present study not only the CIE photopic luminous efficiency function $V(\lambda)$ that is used to calculate (il)luminances from (ir)radiances and which equals the CIE color-matching funtion $\bar{y}$ [6], but also other weighting functions are considered. In detail, two action spectra are used for evaluations in a real-world test scene: the circadian action function describing the melatonin suppression and the photosynthesis action spectrum representing a plant's photosynthesis activity.

Circadian action function

The hormone melatonin, which is mainly secreted during the night, is primarily responsible for the regulation of the circadian rhythm. Light in general and radiation in the blue part of the visible spectrum in particular suppresses the secretion of this hormone. Gall [7] defines a circadian action function $c(\lambda)$ that is based on experimental data from Brainard [8] and Thapan [9] for light-induced melatonin suppression. The spectral distribution of $c(\lambda)$ is shown in Figure 1.

Using this circadian action function, Gall calculates the circadian radiation quantity X_{ec}, which we refer to as C, by

$$C = \int \sigma(\lambda) c(\lambda) d\lambda \tag{1}$$

and defines the circadian action factor a_{cv} in relation to the CIE luminance Y as

$$a_{cv} = \frac{C}{Y} = \frac{\int \sigma(\lambda) c(\lambda) d\lambda}{\int \sigma(\lambda) \bar{y}(\lambda) d\lambda} \tag{2}$$

for a given spectral power distribution (SPD) σ. In the current study we use the values for Gall's circadian action function $c(\lambda)$ that are given in [7] and simulate the distribution of the circadian action factor a_{cv} within a real-world scene.

Photosynthesis action spectrum

Plants as well as some algae and bacteria are able to generate carbohydrates and oxygen from carbon dioxide, water, and light energy. The action spectrum for this photosynthesis process differs for various plants and is subject of scientific research [10, 11].

In the current study we use the photosynthesis action spectrum $sy(\lambda)$ that is defined by the German Institute for Standardization (DIN) in the document DIN 5031-10 [12] and calculate the photosynthesis activity SY from

$$SY = \int \sigma(\lambda) sy(\lambda) d\lambda \tag{3}$$

for a SPD σ. The spectral distribution of $sy(\lambda)$ is shown in Figure 1.

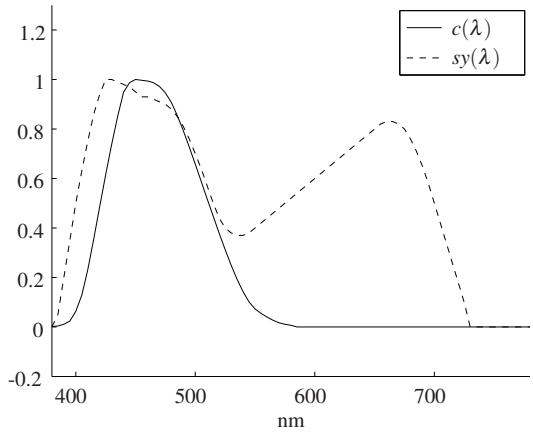

Figure 1. *Spectral distributions of the circadian action function $c(\lambda)$ as defined by Gall and the photosynthesis action spectrum $sy(\lambda)$ as given in DIN 5031-10.*

Spectral Rendering

For spectral rendering with RADIANCE [13, 14] various proposals were presented in the literature. Both Delahunt and Brainard [15] and Ruppertsberg and Bloj [4, 16] use N-step algorithms with multiple calls to the RGB renderer together with a post-processing step to gather the images. Delahunt and Brainard render a single monochromatic image for each wavelength, whereas Ruppertsberg and Bloj put independent wavelengths in each of the three channels. In the latter case wavelengths from the red, green, and blue part of the spectrum should be combined because otherwise the calculation of brightnesses

in RADIANCE given by

$$b(R,G,B) = 0.265 \cdot R + 0.670 \cdot G + 0.0648 \cdot B \quad (4)$$

might lead to inaccuracies in algorithms that are steered by this function. Geisler-Moroder and Dür [5] present an approach for spectral rendering with RADIANCE using a discrete representation of the spectrum with 81 values equally spaced between 380nm and 780nm. They expand the brightness function from the RGB approximation to the CIE tristimulus value Y, i.e.

$$b(\sigma) = Y(\sigma) = \int_{380}^{780} \sigma(\lambda)\bar{y}(\lambda)d\lambda \quad (5)$$

for a SPD σ and the CIE color-matching funtion $\bar{y}$.

For the current study we adopt and slightly modify this approach. Because RADIANCE is intended to be used for simulations of real-world scenes as observed by humans, the brightness function that approximates the CIE Y tristimulus and thus the human brightness perception is used for steering algorithms in the ray tracing process. However, since we use different weighting functions for brightness ($\bar{y}(\lambda)$), melatonin suppression ($c(\lambda)$), and photosynthesis activity ($sy(\lambda)$), we re-define the brightness function in RADIANCE via the constant 1-function as

$$b(\sigma) = \int_{380}^{780} 1 \cdot \sigma(\lambda)d\lambda. \quad (6)$$

In this way all parts of the spectrum are treated equally and inaccuracies in brightness-steered algorithms of RADIANCE are avoided in exchange for a slight computational overhead. In a post-processing step we are then able to apply the sensitivity functions $\bar{y}(\lambda)$, $c(\lambda)$, and $sy(\lambda)$, and compute the indices C, Y, and SY from a single spectral image.

Test scene

Our test scene shows an office room that contains three different sources of illumination – windows, ceiling lamps, and computer monitors. Figure 2 shows an overview of the scene and Figure 3 the view from the the front workplace. The windows are simulated as light sources using the spectrum of the CIE standard illuminant D65 [6] with a luminance of 1000cd/m^2. The spectra of both the TFT display, that emits white light only, and the LED ceiling lamps (Luxeon Rebel cold white) were measured by our cooperation partner Bartenbach LichtLabor [17]. The luminance of the monitors are set to 250cd/m^2 and the ceiling lights are modeled to have a luminous flux of 1500lm each. As for this study primarily the spectrum and not the angular distribution of the light is important, all sources are modeled as totally diffuse emitters. Figure 4 shows the spectra of the three light sources together with the main reflectance spectra of the scene, i.e. the floor, the walls (including the ceiling), and the wooden desks. The reflectance spectra of white plaster (walls, ceiling), cherry wood, and aluminium (e.g. for the ceiling light fixtures) were measured by our cooperation partner Bartenbach LichtLabor. For the other objects we use reflectance spectra from the Macbeth ColorChecker chart [18] that are available on [19], e.g. Macbeth Neutral 6.5 for the floor, Macbeth Foliage for the chairs, and Macbeth Orange and Macbeth Orange Yellow for the containers and their fronts.

Weighting functions

Given a weighting function $\omega(\lambda)$ such as $c(\lambda)$ or $sy(\lambda)$, the associated index $\Omega(\sigma)$ for a spectral power distribution σ is defined by

$$\Omega(\sigma) = \int_{380}^{780} \sigma(\lambda)\omega(\lambda)d\lambda. \quad (7)$$

Figure 2. *Office test scene: overview. The test scene contains three different sources of illumination: four light sources that simulate the windows, two LED ceiling lamps, and two computer monitors.*

Figure 3. *Office test scene: view from the front workplace. This view is important for the evaluation of the circadian action factor a_{cv} as it simulates the field of view of a person working at the desk.*

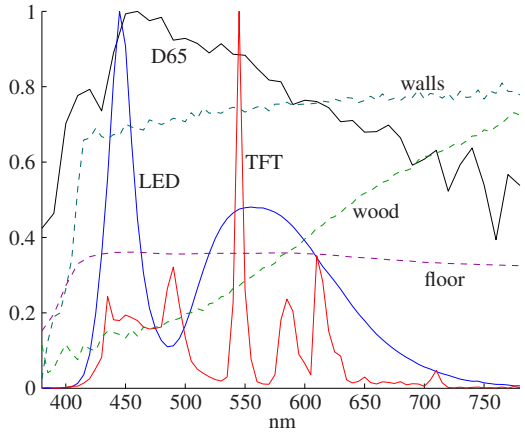

Figure 4. *Light source spectra (each scaled to a maximum of 1) and main reflectance spectra used in the test scene: the windows are modeled with the CIE standard phase of daylight D65, the spectra for the LED lamps and the monitors as well as the reflectances of cherry wood and white plaster were measured by our cooperation partner Bartenbach LichtLabor, and the floor is modeled with the dark gray color Macbeth Neutral 6.5 from the Macbeth ColorChecker chart.*

Thus, Ω becomes a functional on the Hilbert space $L^2([380nm, 780nm])$ that contains all spectra $\sigma(\lambda)$ that

satisfy

$$\int_{380}^{780} \sigma(\lambda)^2 d\lambda < \infty. \tag{8}$$

For example the CIE XYZ tristimulus values can be written as functionals

$$X(\sigma) = \int_{380}^{780} \sigma(\lambda)\bar{x}(\lambda)d\lambda, \tag{9}$$

$$Y(\sigma) = \int_{380}^{780} \sigma(\lambda)\bar{y}(\lambda)d\lambda, \tag{10}$$

$$\text{and} \quad Z(\sigma) = \int_{380}^{780} \sigma(\lambda)\bar{z}(\lambda)d\lambda, \tag{11}$$

where $\bar{x}$, $\bar{y}$, and $\bar{z}$ are the color-matching functions for the CIE 1931 standard colorimetric observer [6] (see Figure 8). Evaluating the functional $Y(\sigma)$ for each pixel's SPD σ in a spectrally rendered image yields the luminance distribution if the image contains radiances, and the illuminance distribution if the image contains irradiances, respectively.

Circadian action function

From the radiances within a spectrally rendered image the circadian action factor a_{cv} can be computed in a post-processing step. For the SPD σ of each pixel the functionals C and Y are evaluated and the circadian action factor

$$a_{cv}(\sigma) = \frac{C(\sigma)}{Y(\sigma)} = \frac{\int_{380}^{780} \sigma(\lambda)c(\lambda)d\lambda}{\int_{380}^{780} \sigma(\lambda)\bar{y}(\lambda)d\lambda} \tag{12}$$

can be displayed in a falsecolor image. Figure 5 shows the distribution of a_{cv} as perceived when working at the front desk. In Figure 6 the a_{cv} values of the scene when seen from outside are presented. In the falsecolor images the a_{cv} values of all three light sources exactly correspond to the analytical results of $a_{cv}(\lambda)$ given in Table 1. Comparing the results for the three light sources shows that the light-induced melatonin suppression is strongest for D65 followed by the TFT monitor light and lastly the LED lamp.

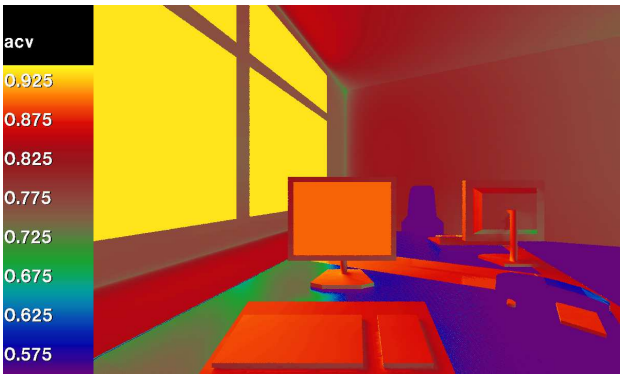

Figure 5. *Distribution of the circadian action factor $a_{cv}(\sigma)$ calculated from the spectral rendering in the field of view of a person working at the front desk.*

Photosynthesis activity

For the photosynthesis activity the incident light is decisive. We thus render the images of our test scene again using the RADIANCE option "-i" to obtain irradiances instead of radiance values. To calculate the photosynthesis index SY from the irradiance spectrum σ at each pixel within the rendered images the

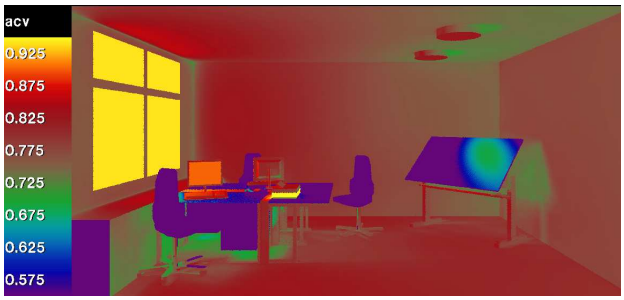

Figure 6. *Distribution of the circadian action factor $a_{cv}(\sigma)$ inside the scene calculated from the spectral rendering. The analytical results for the three light sources given in Table 1 exactly correspond to the image.*

functional $SY(\sigma)$ is evaluated:

$$SY(\sigma) = \int_{380}^{780} \sigma(\lambda)sy(\lambda)d\lambda. \tag{13}$$

Figure 7 shows the SY distribution within the scene and thus proposes the "ideal place" to put plants in the office – on the windowsill or on the desk close to the window. As the index SY is not divided by the brightness of the corresponding SPD it is an absolute measure and depends on both the quality and the quantity of incident light. Thus, the "ideal place" for a plant could for example be changed by increasing the LED's emittance what in turn would lead to uncomfortably high illuminances and glare for the people working in the office.

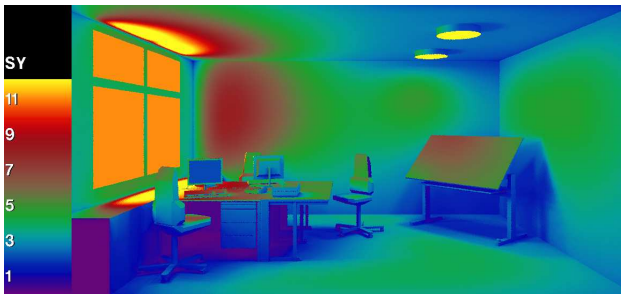

Figure 7. *Distribution of the photosynthesis activity $SY(\sigma)$ inside the scene calculated from the spectral rendering. The windowsill or the parts of the desk close to the window are "ideal places" to position a plant.*

RGB Approximation

In RADIANCE the RGB approximation of luminances and illuminances by Equation 4 usually works well, what is desirable and necessary as these are the main indices needed in lighting design and other applications of this physically based renderer. Similar to the approximation of the CIE tristimulus value Y we try to find an approximation to the indices a_{cv} and SY based on the three color-matching functions $\bar{x}$, $\bar{y}$, and $\bar{z}$.

To calculate the indices C and SY from the values in an RGB rendered image as a weighted sum, we need to derive coefficients (r_C, g_C, b_C) and (r_{SY}, g_{SY}, b_{SY}) for the three channels R, G, and B similar to Equation 4.

Gall and Bieske [20] propose to approximate the circadian action factor a_{cv} via the CIE chromaticity coordinates (x, y) as

$$a_{cv} \approx \frac{\int \bar{z}(\lambda)\sigma(\lambda)d\lambda}{\int \bar{y}(\lambda)\sigma(\lambda)d\lambda} = \frac{Z}{Y} = \frac{1-x-y}{y}. \tag{14}$$

For the light sources in our test scene Equation 14 yields results with relative errors of $+15.7\%$ for D65, $+42.2\%$ for the LED

lamp, and +20.4% for the monitor light. Gall's approximation of the circadian radiation quantity C is only based on the CIE color-matching function $\bar{z}$ and thus leaves room for improvement by calculating an approximation based on all three color-matching functions.

Generally, we look for an approximation of the functional $\Omega(\sigma)$ from Equation 7 by a linear combination

$$\Omega(\sigma) \approx k_x X(\sigma) + k_y Y(\sigma) + k_z Z(\sigma) \tag{15}$$

where $X(\sigma)$, $Y(\sigma)$, and $Z(\sigma)$ are the functionals describing the CIE XYZ tristimuli as given in Equations 9 to 11.

According to the Riesz representation theorem the Hilbert space $L^2([a,b])$ of functions is isomorphic to its dual space of functionals. Thus we can represent each functional Ω by its corresponding density ω and search for an approximation of ω by a linear combination of the color-matching functions $\bar{x}$, $\bar{y}$, and $\bar{z}$, which are the corresponding densities of the functionals X, Y, and Z:

$$\omega(\lambda) \approx k_x \bar{x}(\lambda) + k_y \bar{y}(\lambda) + k_z \bar{z}(\lambda). \tag{16}$$

We find this approximation ψ by an orthogonal projection of ω onto the subspace spanned by $\bar{x}$, $\bar{y}$, and $\bar{z}$, i.e.,

$$\psi = k_x \bar{x} + k_y \bar{y} + k_z \bar{z} \qquad \text{such that} \tag{17}$$

$$\langle \omega - \psi, \bar{x} \rangle = \langle \omega - \psi, \bar{y} \rangle = \langle \omega - \psi, \bar{z} \rangle = 0. \tag{18}$$

Equation 18 leads to the system of linear equations

$$\begin{pmatrix} \langle \omega, \bar{x} \rangle \\ \langle \omega, \bar{y} \rangle \\ \langle \omega, \bar{z} \rangle \end{pmatrix} = G(\bar{x}, \bar{y}, \bar{z}) \cdot \begin{pmatrix} k_x \\ k_y \\ k_z \end{pmatrix} \tag{19}$$

where

$$G(\bar{x}, \bar{y}, \bar{z}) = \begin{pmatrix} \langle \bar{x}, \bar{x} \rangle & \langle \bar{y}, \bar{x} \rangle & \langle \bar{z}, \bar{x} \rangle \\ \langle \bar{x}, \bar{y} \rangle & \langle \bar{y}, \bar{y} \rangle & \langle \bar{z}, \bar{y} \rangle \\ \langle \bar{x}, \bar{z} \rangle & \langle \bar{y}, \bar{z} \rangle & \langle \bar{z}, \bar{z} \rangle \end{pmatrix} \tag{20}$$

is the Gramian matrix for the three color-matching functions $\bar{x}$, $\bar{y}$, and $\bar{z}$. Solving the system (19) for the weighting functions $\omega = c(\lambda)$ and $\omega = sy(\lambda)$ yields the approximations

$$\psi_{c(\lambda)} = -0.284\bar{x} + 0.358\bar{y} + 0.681\bar{z} \quad \text{and} \tag{21}$$

$$\psi_{sy(\lambda)} = 0.533\bar{x} + 0.276\bar{y} + 0.581\bar{z} \tag{22}$$

for the circadian and photosynthesis action spectra, respectively. In Figures 9 and 10 these approximations based on the three CIE color-matching funtions (Figure 8) are compared to the real action functions.

Multiplying by the transformation matrix of RADIANCE from RGB to XYZ gives the coefficients (r,g,b) for the approximation of the index Ω from the RGB values in the rendered image:

$$(r,g,b) = (k_x, k_y, k_z) \cdot \begin{pmatrix} 0.514 & 0.324 & 0.162 \\ 0.265 & 0.670 & 0.0648 \\ 0.0241 & 0.123 & 0.853 \end{pmatrix}. \tag{23}$$

Evaluating Equation 23 for the coefficients of the circadian action spectrum approximation $\psi_{c(\lambda)}$ (Equation 21) and the photosynthesis action spectrum approximation $\psi_{sy(\lambda)}$ (Equation 22) yields the RGB coefficients

$$(r_C, g_C, b_C) = (-0.0346, 0.232, 0.558) \quad \text{and} \tag{24}$$

$$(r_{SY}, g_{SY}, b_{SY}) = (0.361, 0.429, 0.600), \tag{25}$$

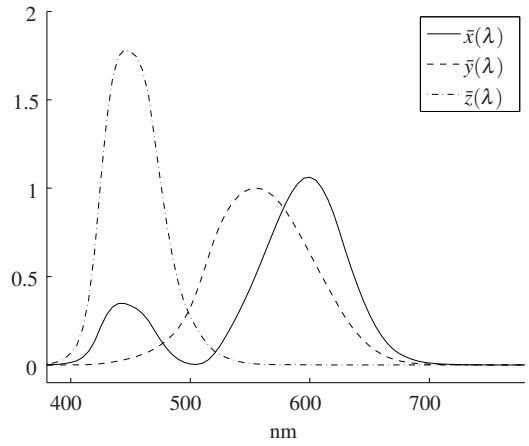

Figure 8. *CIE color-matching functions $\bar{x}$, $\bar{y}$, and $\bar{z}$.*

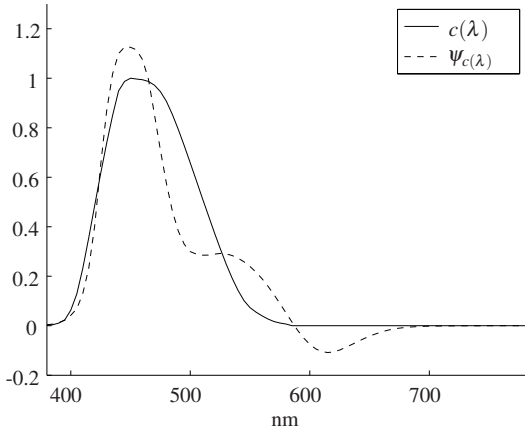

Figure 9. *The circadian action function $c(\lambda)$ as defined by Gall, and the approximation function $\psi_{c(\lambda)}$ that is a linear combination of $\bar{x}$, $\bar{y}$, and $\bar{z}$.*

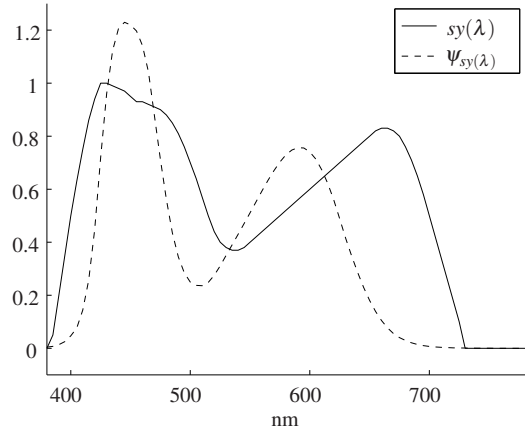

Figure 10. *The photosynthesis action spectrum $sy(\lambda)$ as defined in DIN 5031-10, and the approximation function $\psi_{sy(\lambda)}$ as a linear combination of $\bar{x}$, $\bar{y}$, and $\bar{z}$.*

respectively. Finally, the approximations for the circadian action

factor a_{cv} and the photosynthesis activity SY are given by

$$a_{cv}(R,G,B) = \frac{C(R,G,B)}{b(R,G,B)} = \frac{-0.0346 \cdot R + 0.232 \cdot G + 0.558 \cdot B}{0.265 \cdot R + 0.670 \cdot G + 0.0648 \cdot B} \tag{26}$$

and

$$SY(R,G,B) = 0.361 \cdot R + 0.429 \cdot G + 0.600 \cdot B. \tag{27}$$

In Table 1 the analytical results for the three light sources in the test scene (D65, LED, monitor light) are presented. The correct values for the circadian action factor a_{cv} and the photosynthesis activity SY are opposed to their RGB approximations. Additionally, the relative errors of the RGB approximations are given. For both indices a_{cv} and SY the RGB approximation performs best for the LED illuminant, followed by the monitor light and lastly the CIE phase of daylight D65. However, even for the LED lamp the relative error for the circadian action index is already greater than 5%.

	D65	LED	TFT
$a_{cv}(\sigma)$	0.941	0.824	0.903
$a_{cv}(R,G,B)$	0.830	0.871	0.834
Δa_{cv}	-11.82%	+5.72%	-7.69%
$SY(\sigma)$	2.198	6.400	0.415
$SY(R,G,B)$	1.581	6.333	0.393
ΔSY	-28.05%	-1.04%	-5.40%

Table 1. *Analytical results for the three light sources used in the test scene. The correct values of the circadian action factor $a_{cv}(\sigma)$ and the photosynthesis activity $SY(\sigma)$ are opposed to the RGB approximations $a_{cv}(R,G,B)$ and $SY(R,G,B)$, respectively. Additionally, the particular relative error Δ is depicted.*

Re-rendering the scene with the standard RGB version of RADIANCE yields an RGB color value for each pixel describing the radiance or irradiance distribution within the test scene. To calculate the approximation for the circadian action factor a_{cv} Equation 26 is evaluated for the RGB radiance values of each pixel. The results are presented as falsecolor images in Figure 11 for the computer workplace view and in Figure 12 for the scene overview as seen from outside, each on the left side. The images on the right side in Figures 11 and 12 show the relative differences in percent between the correct results for a_{cv} calculated from the spectral renderings (Figures 5 and 6) and the RGB approximations, i.e.

$$\Delta a_{cv} = 100 \cdot \frac{a_{cv}(R,G,B) - a_{cv}(\sigma)}{a_{cv}(\sigma)}. \tag{28}$$

The values for both $a_{cv}(R,G,B)$ and Δa_{cv} for the three light sources D65, LED, and the monitor light comply with the analytical values in Table 1.

Evaluating Equation 27 for the irradiance color values of each pixel obtained from the RGB rendering with the option "-i" yields an approximation for the photosynthesis activity SY at the particular pixel, i.e., the position in the scene. Figure 13 shows the RGB approximation for SY opposed to the relative differences in percent between the correct results from the spectral rendering (Figure 7) and the RGB approximation, calculated as

$$\Delta SY = 100 \cdot \frac{SY(R,G,B) - SY(\sigma)}{SY(\sigma)}. \tag{29}$$

Again, the analytical results for $SY(R,G,B)$ and ΔSY for the three light sources exactly correspond to the values in Table 1.

One idea to improve the performance of the approximations is to consider all spectra only on the constrained domain where the action spectra are non-zero. For example the values of the melatonin suppression function are non-zero in the interval from 380nm to 580nm. From Equations 16 to 20 an approximation formula for $a_{cv}(\sigma)$ similar to Equations 21 and 26 can be derived that shows smaller relative errors when compared to the values given in Table 1. However, we could not use this approach directly within our RGB renderings as some of the truncated spectra lead to negative RGB input values and the gamut clipping of these RGB triples yields approximations that are worse than those presented in Figures 11 and 12. For the photosynthesis action spectrum the approach based on the constrained interval from 385nm to 725nm does not improve the approximation because all three color-matching functions $\bar{x}$, $\bar{y}$, and $\bar{z}$ are close to zero outside of this domain.

Conclusion

We have shown how indices derived from various weighting functions such as the circadian action factor or the photosynthesis activity can be calculated within spectrally rendered images. Based on the CIE color-matching functions we presented approximations to calculate the indices a_{cv} and SY from RGB rendered images. However, as these RGB approximations turned out to be rough estimations, we propose to use spectral rendering whenever accurate results are desired. If no spectral rendering engine is available, the methods proposed by Delahunt and Brainard [15] and Ruppertsberg and Bloj [16] could be used to perform spectral rendering using the standard RGB version of the RADIANCE rendering engine.

Acknowledgments

The authors thank Christian Knoflach and Rico Thetmeyer from our cooperation partner Bartenbach LichtLabor in Aldrans, Austria, for the office test scene and the associated photometric data. The reviewers' comments that helped to improve this paper are gratefully acknowledged. Parts of this research were supported by the FIT-IT Program of the BMVIT (Bundesministerium für Verkehr, Innovation und Technologie) and the FFG with Grant No. 816009.

References

[1] John Mardaljevic, Daylight Simulation: Validation, Sky Models and Daylight Coefficients, PhD thesis, De Montfort University, Leicester, Institute of Energy and Sustainable Development, 1999.

[2] Christiane Ulbricht, Alexander Wilkie, and Werner Purgathofer, Verification of Physically Based Rendering Algorithms, in State of the Art Reports, Eurographics 05, 95-112, 2005.

[3] David Geisler-Moroder and Arne Dür, Validation of Radiance against CIE171:2006 and Improved Adaptive Subdivision of Circular Light Sources, 7th International RADIANCE Workshop, Fribourg, Switzerland, 2008.

[4] Alexa I. Ruppertsberg and Marina Bloj, Rendering complex scenes for psychophysics using RADIANCE: How accurate can you get?, J. Opt. Soc. Am. A, 23, 4, 759-768, 2006.

[5] David Geisler-Moroder and Arne Dür, Color-rendering indices in global illumination methods, Journal of Electronic Imaging, 18, 4, 043015-1–043015-12, 2009.

[6] CIE, Colorimetry, 3rd ed., CIE Publication 15:2004, 2004.

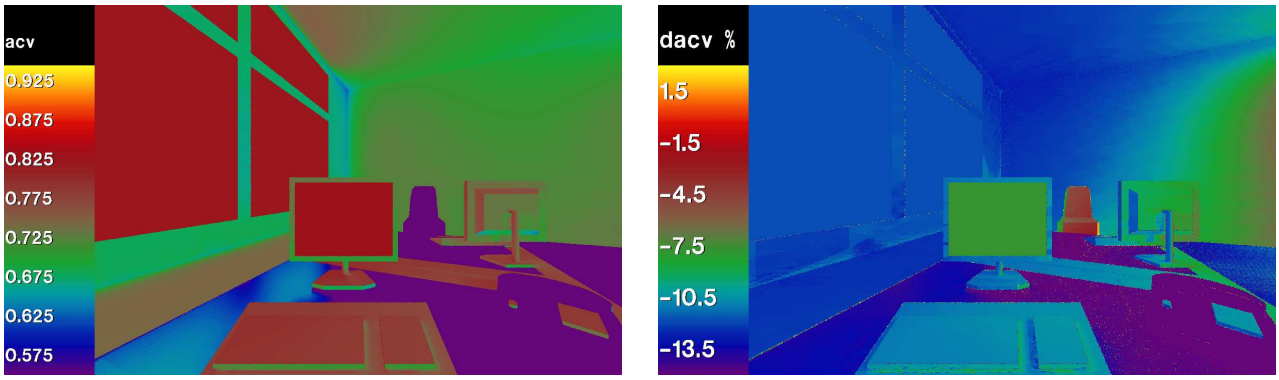

(a) (b)

Figure 11. *(a) Distribution of the approximated circadian action factor $a_{cv}(R,G,B)$ calculated from the RGB rendering using Equation 26 in the field of view as perceived by a person working at the front desk and (b) resulting relative differences Δa_{cv} from the values obtained from the spectral rendering.*

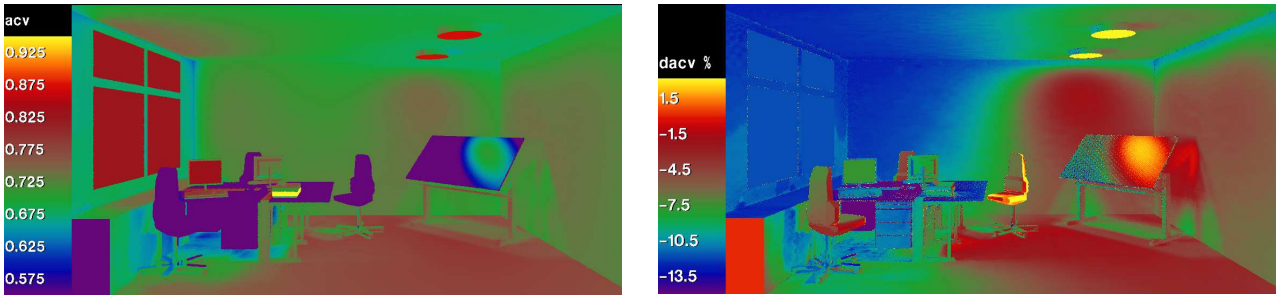

(a) (b)

Figure 12. *(a) Distribution of the approximated circadian action factor $a_{cv}(R,G,B)$ inside the scene calculated from the RGB rendering using Equation 26 and (b) resulting relative differences Δa_{cv} from the values obtained from the spectral rendering.*

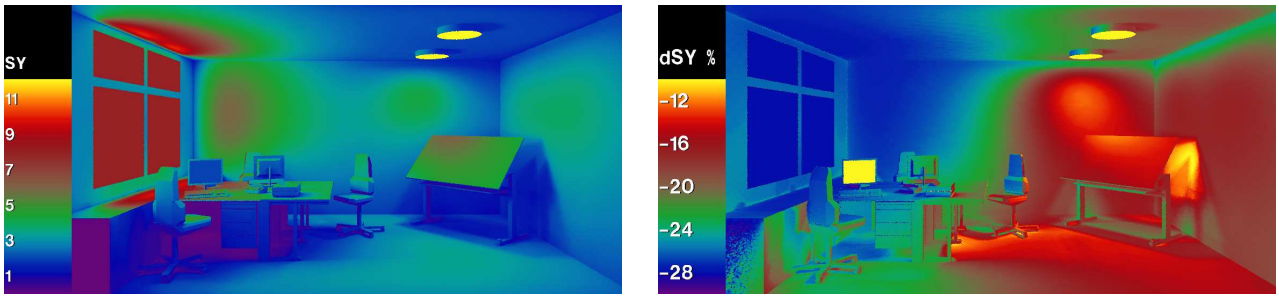

(a) (b)

Figure 13. *(a) Distribution of the approximated photosynthesis activity $SY(R,G,B)$ inside the scene calculated from the RGB rendering using Equation 27 and (b) resulting relative differences ΔSY from the values obtained from the spectral rendering.*

[7] Dietrich Gall, Die Messung circadianer Strahlungsgrößen, online: www.tu-ilmenau.de/fakmb/fileadmin/template/fglt/publikationen/2004/Vortrag_Gall2004.pdf, 11/07/2009.

[8] George C. Brainard et al., Action Spectrum for Melatonin Regulation in Humans: Evidence for a Novel Circadian Photoreceptor, The Journal of Neuroscience 21(16), 6405-6412, 2001.

[9] Kavita Thapan, Josephine Arendt, and Debra J. Skene, An action spectrum for melatonin suppression: evidence for a novel non-rod, non-cone photoreceptor system in humans, Journal of Physiology 535.1, 261-267, 2001.

[10] Shinji Tazawa, Effects of Various Radiant Sources on Plant Growth (Part 1), Japan Agricultural Research Quarterly, 33, 3, 163–176, 1999.

[11] Shinji Tazawa, Effects of Various Radiant Sources on Plant Growth (Part 2), Japan Agricultural Research Quarterly, 33, 3, 177–183, 1999.

[12] DIN 5031-10, Optical radiation physics and illuminating engineering - Part 10: Photobiologically effective radiation, quantities, symbols and actions.

[13] Gregory J. Ward, The RADIANCE lighting simulation and rendering system, in SIGGRAPH '94 Proceedings, (New York, NY, USA), 459-472, ACM, 1994.

[14] Greg Ward and Rob Shakespeare, Rendering with Radiance, Morgan Kaufmann Publishers, 1998.

[15] Peter B. Delahunt and David H. Brainard, Does human color constancy incorporate the statistical regularity of natural daylight?, Journal of Vision, 4, 2, 57-81, 2004.
[16] Alexa I. Ruppertsberg and Marina Bloj, Creating physically accurate visual stimuli for free: Spectral rendering with RADIANCE, Behavior Research Methods, 40, 1, 304-308, 2008.
[17] Bartenbach LichtLabor, Homepage, www.bartenbach.com.
[18] C. S. McCamy, H. Marcus, and J. G. Davidson, A Color-Rendition Chart, Journal of Applied Photographic Engineering, 20, 3, 95-99, 1976.
[19] BabelColor, ColorChecker data, www.babelcolor.com/download/ColorChecker_RGB_and_spectra.xls, 11/07/2009.
[20] Dietrich Gall and Karin Bieske, Definition and Measurement of Circadian Radiometric Quantities, in Light and health – non-visual effects: Proc. of the CIE Symposium '04, 2004.

Author Biography

David Geisler-Moroder received his Diploma degree in Technical Mathematics from the University of Innsbruck, Austria, in 2006. For his thesis on color rendering and color differences he was awarded the scientific prize of the Federal Economic Chamber of Tyrol. He is currently pursuing his PhD degree at the Department of Mathematics at the University of Innsbruck, where he is a research fellow in a project on Visual Computing. His main research interests include physically based rendering, global illumination, and colorimetry.

Arne Dür received his Diploma and PhD degrees in mathematics from the University of Innsbruck, Austria, in 1981 and 1983. He is currently an associate professor at the Department of Mathematics of the University of Innsbruck. His primary research interests include discrete mathematics and computer graphics.